Soliton oscillation driven by spin-orbit coupling in spinor condensates

Decheng Ma and Chenglong Jia*

Key Laboratory for Magnetism and Magnetic Materials of the Ministry of Education & School of Physical Science and Technology, Lanzhou University, Lanzhou 730000, China

(Received 29 March 2019; published 27 August 2019)

We theoretically investigate the dynamics of polar bright soliton under the influence of spin-orbit coupling (SOC) in spin-1 three component Bose-Einstein condensate (BEC). Periodically oscillating dark-bright-dark solitons are found to be induced by the SOC with their multifrequency oscillations jointly determined by the interparticle nonlinear interaction and the SOC strength. Explicit formulas are provided to identify these frequencies, which are in good agreement with the numerical simulation results. A linear Zeeman interaction is further introduced to break the time-reversal symmetry and change the polarity of the spinor BECs, which results in the periodic transition of the system from polar state to ferromagnetic state.

DOI: 10.1103/PhysRevA.100.023629

I. INTRODUCTION

Solitons are topological stable excitations, which exist in a variety of fields and play an important role in communication technologies [1]. Since the realization of Bose-Einstein condensate (BEC), this intrinsically nonlinear system provides a versatile test bed for soliton studies [2–4]. There are many different methods and experimental technologies to generate solitons in BECs, which allowed both bright and dark solitons to be extensively investigated [5–20]. In multicomponent BECs, the high number of degrees of freedom leads to a rich dynamics: dark-bright solitons [14,21–24] and dark-antidark solitons [25] have been created in two-component BECs. With the aid of intercomponent interaction, solitons of dark-bright-bright and dark-dark-bright types have been generated in spin-1 BECs as well [26]. On the other hand, since the realization of synthetic magnetic field in BECs, artificial spin-orbit coupling (SOC) has been generated in multicomponent BECs [27–34]. Under the influence of SOC, solitons show exotic density profile and nontrivial dynamics [35–43]. As demonstrated in Ref. [43], the SOC can exert influence on the soliton dynamics, resulting in an oscillating behavior in two-component BECs. Effectively, by a unitary transformation, SOC can be transformed into an effective coupling between different components of spinor BECs [39], which would lead particle exchange among different components. However, the effects of SOC on the structure and dynamic evolution of soliton is still not fully appreciated, in particular in the spinor BECs [26].

In the present paper, by using SOC as an effective intercomponent interaction to transfer particle between three different components of spin-1 BECs, dark-bright-dark solitons are generated from an initial polar bright soliton and show the periodic oscillations. In particular, two oscillation frequencies are identified: one is determined by the nonlinear spin-independent interaction and another one is related to the SOC strength. After including the linear Zeeman interaction, the oscillation patterns are modified and additional spin-polarization oscillations are induced in the system with the spinor BECs changing periodically between polar state and ferromagnetic state. In addition, the related manifold mixing dynamics in our system is corroborated by direct numerical simulations [44].

II. SOLITON DYNAMICS

We consider a dilute gas of bosonic atoms with hyperfine spin $F = 1$ in one-dimensional system under the influence of the Rashba-type SOC. The corresponding Hamiltonian is given by

$$H = \int dx \left\{ \Psi^\dagger \left[-\frac{\hbar^2}{2m}\nabla^2 - \alpha k \cdot \hat{f}_y \right] \Psi + \frac{c_0}{2}|\rho|^2 + \frac{c_2}{2}|\mathbf{F}|^2 \right\}, \tag{1}$$

where $\Psi(x,t) = (\psi_1, \psi_0, \psi_{-1})^T$ is the mean-field order parameter and the wave functions are normalized $\int dx(|\psi_1|^2 + |\psi_0|^2 + |\psi_{-1}|^2) = 1$. α describes the strength of the SOC, $\mathbf{F} = \sum_{\mathrm{m}} \psi^*_{\mathrm{m}} \hat{f}_{\mathrm{mn}} \psi_{\mathrm{n}}$ is the spin-polarization vector with the spin-1 matrices $\hat{f}_{\mathrm{i}}$ $(i = x, y, z)$, and $\rho = \sum_{\mathrm{m}} |\psi_{\mathrm{m}}|^2$ is the total density of atoms. $c_0 = (g_0 + 2g_2)/3$ and $c_2 = (g_2 - g_0)/3$ denote the effective spin-independent and spin-exchange interaction constants, respectively. Here $g_{\mathrm{F}} = 4\pi\hbar^2 a_{\mathrm{F}}/M$ $(F = 0,\ 2)$ are the coupling constants for different spin channel with the s-wave scattering length a_{F}.

The dynamics of the system is described by the coupled Gross-Pitaevskii equations (GPE). By rescaling the time and length in units of $\hbar/|c_0|$ and $\sqrt{\hbar^2/m|c_0|}$, respectively, the GPEs can be rewritten in the dimensionless form:

$$i\frac{\partial \tilde{\psi}_1}{\partial t} = [\mathcal{L} + \tilde{c}_2(|\tilde{\psi}_1|^2 + |\tilde{\psi}_0|^2 - |\tilde{\psi}_{-1}|^2)]\tilde{\psi}_1 + \tilde{c}_2\tilde{\psi}_0^2\tilde{\psi}_{-1}^* + \frac{\tilde{\alpha}}{\sqrt{2}}\partial_{\mathrm{x}}\tilde{\psi}_0,$$

*cljia@lzu.edu.cn

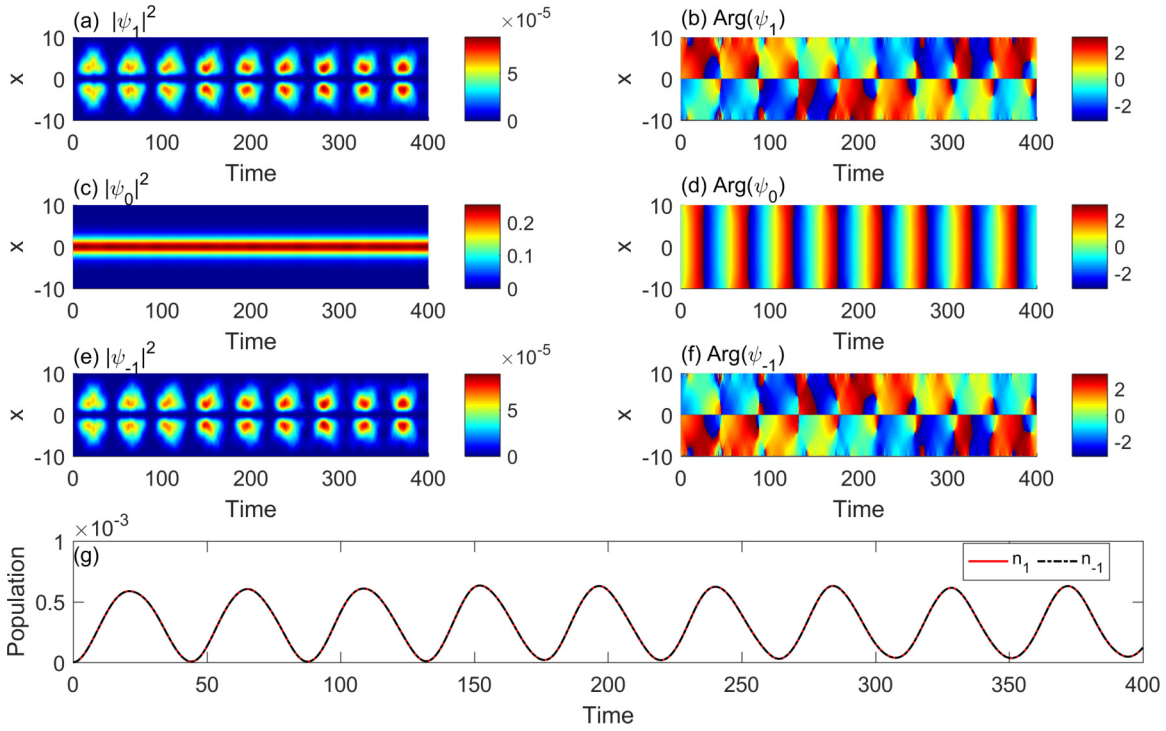

FIG. 1. Evolution of the polar soliton in spinor BECs with time under the perturbation of small SOC with the parameters $c_0 = -1, c_2 = 1, k = 0.5, A = 0.5$, and $\alpha = 0.01$. The time evolutions of density distribution (a), (c), (e) and the corresponding phase (b), (d), (f) of $\psi_1, \psi_0, \psi_{-1}$ are shown in the respective figures. The particle population of $\psi_{\pm 1}$ is presented in (g).

$$
\begin{aligned}
i\frac{\partial\tilde{\psi}_0}{\partial t} &= [\mathcal{L} + \tilde{c}_2(|\tilde{\psi}_1|^2 + |\tilde{\psi}_{-1}|^2)]\tilde{\psi}_0 \\
&\quad + 2\tilde{c}_2\tilde{\psi}_0^*\tilde{\psi}_1\tilde{\psi}_{-1} - \frac{\tilde{\alpha}}{\sqrt{2}}(\partial_x\tilde{\psi}_1 - \partial_x\tilde{\psi}_{-1}), \\
i\frac{\partial\tilde{\psi}_{-1}}{\partial t} &= [\mathcal{L} + \tilde{c}_2(|\tilde{\psi}_{-1}|^2 + |\tilde{\psi}_0|^2 - |\tilde{\psi}_1|^2)]\tilde{\psi}_{-1} \\
&\quad + \tilde{c}_2\tilde{\psi}_0^2\tilde{\psi}_1^* - \frac{\tilde{\alpha}}{\sqrt{2}}\partial_x\tilde{\psi}_0,
\end{aligned} \tag{2}
$$

where $\tilde{\psi}_F = \sqrt[4]{\hbar^2/m|c_0|}\psi_F$, $\tilde{c}_0 = \mathrm{sgn}(c_0), \tilde{c}_2 = c_2/|c_0|$, $\tilde{\alpha} = \alpha\sqrt{m/\hbar^2|c_0|}$, and $\mathcal{L} = -\frac{1}{2}\nabla^2 + \tilde{c}_0(|\tilde{\psi}_1|^2 + |\tilde{\psi}_0|^2 + |\tilde{\psi}_{-1}|^2)$. In the following discussion, for simplicity, we omit the tilde of all renormalized parameters.

From a symmetry point of view, in the absence of SOC, the Hamiltonian is invariant under the global U(1) gauge transformation, the SO(3) rotation in spin space, and the time reversal transformation $\mathcal{T} \equiv \exp(-i\pi\hat{f}_y)\mathcal{K}$ [45,46]. After including the SOC interaction, the symmetry of the system is reduced by requiring invariance under simultaneous rotation in the spin space and real space [45]. Therefore, with more degree of freedom and internal symmetry breaking, the spinor BECs can hold more complex structure and sophisticated dynamics. Reference [38] revealed that the system without SOC can support both polar soliton $(\psi_1, \psi_0, \psi_{-1}) = \sqrt{-\mu}\,\mathrm{sech}(\sqrt{-\mu}x)\exp(-i\mu t)(\epsilon, \sqrt{1-\epsilon^2}, \epsilon)$ and ferromagnetic bright soliton solutions $(\psi_1, \psi_0, \psi_{-1}) = [\sqrt{2\mu/(c_0+c_2)}\,\mathrm{sech}(\sqrt{-\mu}x)\exp(-i\mu t), 0, 0]$, where μ is the corresponding chemical potential and ϵ is an arbitrary parameter taking values $-1 < \epsilon < 1$, respectively. In the presence of SOC interaction [39], the polar soliton state is modified to be $(\psi_1, \psi_0, \psi_{-1}) = A[\varepsilon\cos(\alpha x) + \sqrt{1/2+\sqrt{2}\varepsilon^2}\sin(\alpha x), -\sqrt{2}\varepsilon\sin(\alpha x) + \sqrt{1-2\varepsilon^2}\cos(\alpha x), -\varepsilon\cos(\alpha x) - \sqrt{1/2+\sqrt{2}\varepsilon^2}\sin(\alpha x)]\mathrm{sech}(kx)$, where $\varepsilon \in [0, 1/2]$. In this study, we choose the polar bright soliton $(\psi_1, \psi_0, \psi_{-1}) = A(0, \mathrm{sech}(kx), 0)$ with $\alpha = 0$ as our initial state [38,39], and then we switch on α to investigate the influence of SOC on soliton dynamics.

By numerically solving Eq. (2) [44], we get the evolutions of initial polar soliton state with parameters $c_0 = -1, c_2 = 1$ under small SOC interaction $\alpha = 0.01$. The k parameter was determined by the relation $k^2 = -c_0A^2$ and takes the value $k = 0.5$ by the normalization relation $\int dx(|\psi_1|^2 + |\psi_0|^2 + |\psi_{-1}|^2) = 1$ in our system. Both the density [Figs. 1(a), 1(c), and 1(e)] and corresponding phase [1(b), 1(d), 1(f)] of each component ψ_1, ψ_0, ψ_{-1} are reported. In Fig. 1(g), we also show variations of the particle population $(n_{\pm 1})$ of $\psi_{\pm 1}$ with time. One can see that the SOC does not change the polarity of the system. ψ_1 and ψ_{-1} have equal density and conjugated phase distribution. Additionally, as indicated by the notches in the middle of $\psi_{\pm 1}$ components with abrupt phase change at $x = 0$ in Figs. 1(b) and 1(f), the $\psi_{\pm 1}$ components behave as two periodically oscillating dark solitons. Comparing these with the random perturbed soliton in Ref. [38], it can be observed that the SOC induced soliton presents a more complex structure and it can be probably used as a way to generate dark solitons in spinor BECs. Furthermore, as suggested in Ref. [47], the hollow channel in the middle of $\psi_{\pm 1}$ can effectively serve as a waveguide for the ψ_0 component, which is a useful way to construct soliton waveguides.

The oscillating behaviors identified can be understood within the linear response theory. Given that the SOC interaction is quite weak, by retaining the linear terms of $\psi_{\pm1}$ in the GPEs and taking into account the relation $\psi_{-1} = -\psi_1^*$ and $\psi_0^* = \psi_0$ in the polar state, we get the effective dynamic equations for $\psi_{\pm1}$,

$$i\frac{\partial\psi_{\pm1}}{\partial t} = -\frac{1}{2}\nabla^2\psi_{\pm1} + c_0|\psi_0|^2\psi_{\pm1} \pm \frac{\alpha}{\sqrt{2}}\partial_x\psi_0. \quad (3)$$

As shown in Fig. 1, the ψ_0 component of the spinor BECs in the presence of weak SOC is mainly distributed around the center of the system [$\sim$sech(kx)]; hence we can characterize ψ_0 with its initial value at $x = 0$ and take an approximation $\partial_x\psi_0|_{x=0} \approx 0$. Subsequently, one obtains the simplified equations,

$$i\partial_t\psi_{\pm1} = \left(c_0|A|^2 + \frac{k^2}{2}\right)\psi_{\pm1}, \quad (4)$$

by which the effective oscillating frequency $\omega_1 \approx |c_0A^2 + \frac{k^2}{2}|$ is obtained. After introducing the parameters used in Fig. 1, we have $\omega_1 \approx 0.125$. The corresponding period is then obtained $T = 2\pi/\omega_1 \approx 50$, which is in agreement with the numerical simulations. However, it should be noted that the SOC α does not explicitly appear in the effective frequency ω_1; however, it is a crucial driven source to have small, but nonzero $\psi_{\pm1}$.

When the SOC strength is comparable with the nonlinear interaction strength c_F, the hybridization induced by the SOC becomes strong and the linear response theory cannot be applied. By considering the symmetry of the system and taking a gauge transformation $\Psi = \exp(i\alpha\hat{f}_y x)\bar{\Psi}$ [39], we get the transformed GPEs,

$$i\frac{\partial\bar{\psi}_m}{\partial t} = -\frac{1}{2}\nabla^2\bar{\psi}_m + c_0\rho\bar{\psi}_m + c_2\sum_n \mathbf{F}\cdot\mathbf{f}_{mn}\bar{\psi}_n - \frac{1}{2}\alpha^2\sum_n (f_y^2)_{mn}\bar{\psi}_m, \quad (5)$$

where

$$f_y^2 = \frac{1}{2}\begin{pmatrix} 1 & 0 & -1 \\ 0 & 2 & 0 \\ -1 & 0 & 1 \end{pmatrix}.$$

Clearly, SOC as a new term leads to additional coupling between $\bar{\psi}_{\pm1}$ components, which is expected to result in an additional oscillation of the system.

The dynamic evolution of the system with the SOC strength $\alpha = \sqrt{2}$ is displayed in Fig. 2. Although the polar property of the system is still entirely maintained with equal densities of $\psi_{\pm1}$, the initial bright soliton has been completely destroyed by the strong SOC and the condensates oscillate with two frequencies. The fast oscillations can be understood with a heuristic argument using the function ψ_0. By focusing on the center of the system, we can roughly neglect the x distribution of ψ_0; further, with $\psi_{\pm1}$ vanishing in the middle of the system, we have an effective equation of $\bar{\psi}_0$,

$$i\frac{\partial\bar{\psi}_0}{\partial t} = c_0|\bar{\psi}_0|^2\bar{\psi}_0 - \frac{1}{2}\alpha^2\bar{\psi}_0. \quad (6)$$

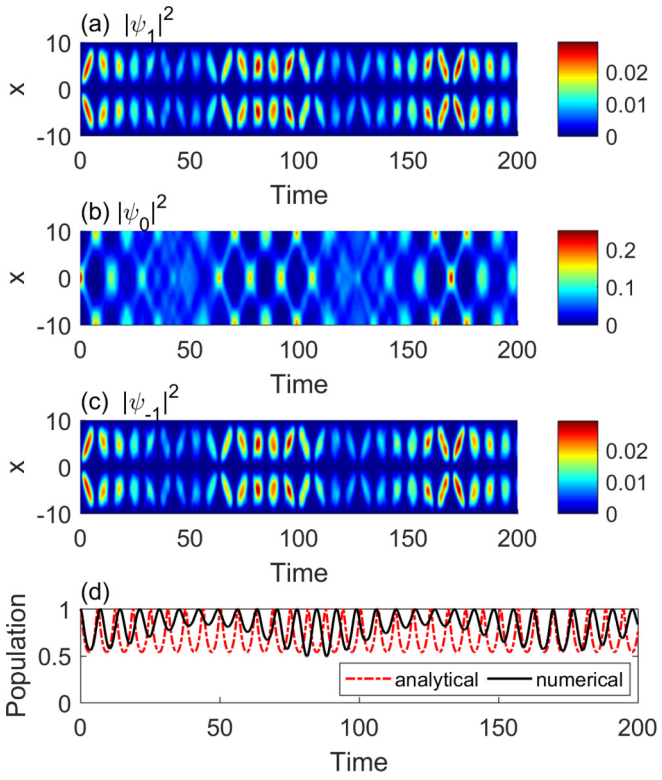

FIG. 2. When the SOC is comparable with the interparticle interaction, the initial bright soliton structure cannot be held. The density evolution of ψ_1 (a), ψ_0 (b), and ψ_{-1} (c) shows multifrequencies oscillations. In (d), the particle population $n_0 = \int|\psi_0|^2dx$ is given by the numerical simulations (black line) and the analytical formula [Eq. (8), red dot line]. The parameters were set to be $c_0 = -1$, $c_2 = 1$, $k = 0.5$, $A = 0.5$, and $\alpha = \sqrt{2}$.

With the initial value $\bar{\psi}_0(0) = A$, we propose a trial solution $\bar{\psi}_0 = \exp(-i\delta t)f$, where $\delta = -\alpha^2A/2$ accounts for the phase shift induced by the SOC. Substituting this ansatz into Eq. (6), the equation of motion of f reads

$$i\partial_t f = c_0f^3 - \tfrac{1}{2}\alpha^2(1-A)f. \quad (7)$$

Taking the initial normalization constant $A = 1/2$, the above equation deduces an analytical solution

$$f(t) = \frac{\alpha\,\exp(i\alpha^2t/4)}{2\sqrt{\alpha^2 + c_0\exp(i\alpha^2t/2) - c_0}}. \quad (8)$$

As shown in Fig. 2(d), the higher frequency oscillations given by Eq. (8) are in good agreement with the numerical simulations of ψ_0. On the other hand, the low frequency ω_1, determined by the interaction c_0, is now further reduced by the smaller ψ_0 density; because of a stronger SOC interaction, a longer periodicity (>50) is expected in the dynamic evolution of the system. The low and high frequencies jointly result in the multifrequency modulated fringe patterns in Fig. 2. On the other hand, the SOC induced particle transfer between different components is closely linked to the spin-mixing dynamics in SOC spinor BECs [48,49]. Please note that the oscillation and dark-bright-dark soliton structure induced by SOC are quite different from the dynamics of the soliton in Ref. [39], which are the eigenstates of the SOC spin-1 BECs.

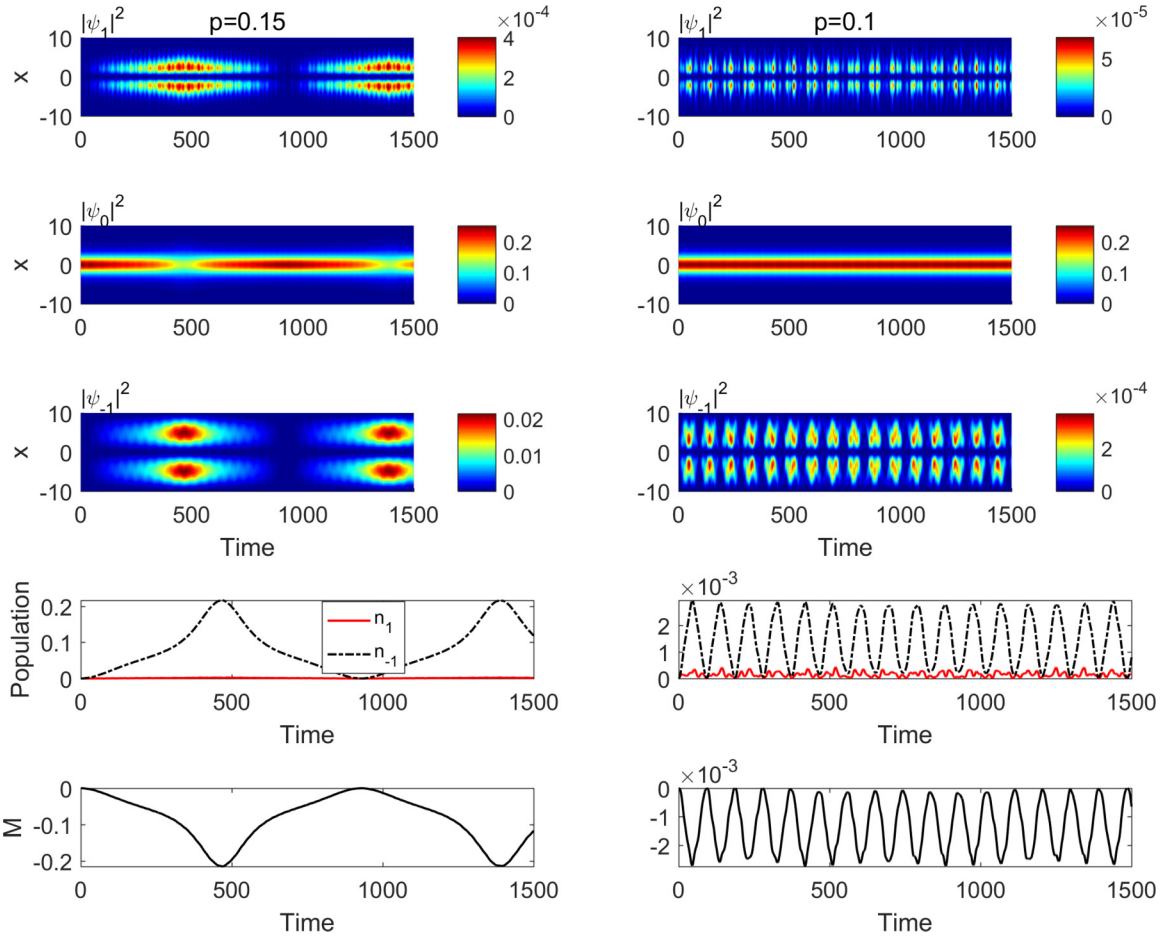

FIG. 3. By applying an external magnetic field, the additional linear Zeeman term results in an unbalanced density distribution between $\psi_{\pm1}$ components and the system becomes polarized. The variations of the density distribution, the particle population $n_{\pm1}$, and the induced magnetization M over time in the presence of $p = 0.15, 0.1$ are presented, respectively. The rest parameters are set to be $\alpha = 0.01$, $c_0 = -1$, $c_2 = 1$, $k = 0.5$, and $A = 0.5$.

III. POLARIZATION TRANSITION

As demonstrated by Figs. 1 and 2, with only SOC, the oscillating transition between three components does not destroy the polarity of the system. In order to have a nonzero polarization (magnetization) in the spinor BECs, we introduce a linear Zeeman term into the GPEs, which would break the time-reversal symmetry and lead to an unbalanced density distribution between $\psi_{\pm1}$ components, and hence the condensates could change from the polar state to the ferromagnetic state:

$$\begin{aligned} i\frac{\partial\psi_1}{\partial t} &= [\mathcal{L} + c_2(|\psi_1|^2 + |\psi_0|^2 - |\psi_{-1}|^2)]\psi_1 \\ &\quad + p\psi_1 + c_2\psi_0^2\psi_{-1}^* + \frac{\alpha}{\sqrt{2}}\partial_x\psi_0, \\ i\frac{\partial\psi_0}{\partial t} &= [\mathcal{L} + c_2(|\psi_1|^2 + |\psi_{-1}|^2)]\psi_0 \\ &\quad + 2c_2\psi_0^*\psi_1\psi_{-1} - \frac{\alpha}{\sqrt{2}}(\partial_x\psi_1 - \partial_x\psi_{-1}), \\ i\frac{\partial\psi_{-1}}{\partial t} &= [\mathcal{L} + c_2(|\psi_{-1}|^2 + |\psi_0|^2 - |\psi_1|^2)]\psi_{-1} \\ &\quad - p\psi_{-1} + c_2\psi_0^2\psi_1^* - \frac{\alpha}{\sqrt{2}}\partial_x\psi_0. \end{aligned} \tag{9}$$

Given a positive p, in comparison to the ψ_1 component, ψ_{-1} becomes more energetically favored, which results in higher particle population in the ψ_{-1} component, with the system becoming polarized. Such polarization of the system can be described by an effective magnetization given by $M = \int dx\, F_z = \int dx(|\psi_1|^2 - |\psi_{-1}|^2)$.

As one can see from Fig. 3, in the presence of the linear Zeeman field $p = 0.1, 0.15$ and the SOC $\alpha = 0.01$, the system indeed becomes polarized with more particles populated in the ψ_{-1} component. The spatial distribution of ψ_1 and ψ_{-1} becomes no longer symmetric at all, while the ψ_0 component is still mainly distributed in the middle of the system. The peak splitting of $\psi_{\pm1}$ becomes even more complex as the p increases. More importantly, one can notice that the induced magnetization is dramatically enhanced by several orders as the Zeeman field changes a little bit, from $p = 0.1$ to $p = 0.15$.

Since $n_{-1} \gg n_1$ in the polarized phase, we have then $M \approx -n_{-1}$. Multiplying the GPEs with ψ_{-1}^* and integrating over the space, we get an effective dynamic equation of M,

$$i\partial_t M = -2(c_0 + c_2 - p)M + \mathcal{S}. \tag{10}$$

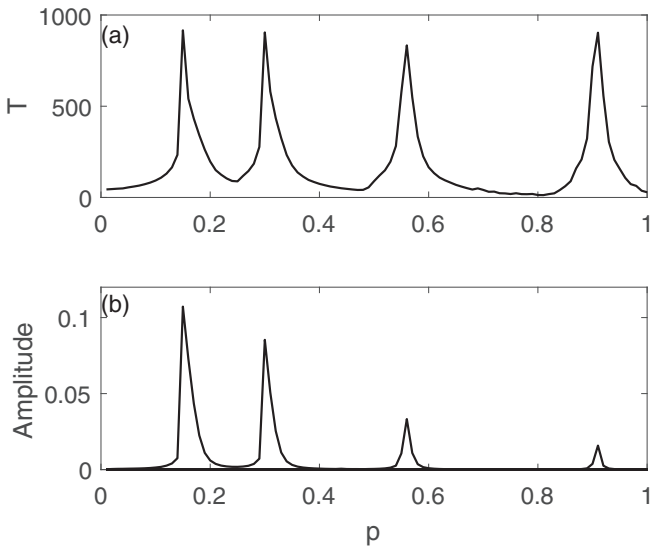

FIG. 4. Fundamental oscillating period T (a) and the amplitude (b) of the induced magnetization M versus the linear Zeeman field p. Four resonant peaks locate at $p = 0.15, 0.3, 0.56, 0.91$, respectively.

Here, the parameter $\mathcal{S}$ is given by $\mathcal{S} = \int dx[\frac{1}{2}[\psi_{-1}^*\nabla^2\psi_{-1} - (\nabla^2\psi_{-1}^*)\psi_{-1}] - c_2(\psi_{-1}^*\psi_0^2\psi_1^* - \psi_0^{*2}\psi_1\psi_{-1}) + \frac{\alpha}{\sqrt{2}}\ [\psi_{-1}^*\ \ \partial_x\psi_0 - (\partial_x\psi_0^*)\psi_{-1}]]$. Let us suppose that $\mathcal{S}$ is negligibly small and the dynamics of M is dominated by the first term in Eq. (10); the magnetization M would oscillate with time and its frequency would linearly increase with the Zeeman field p. However, detailed calculations show that the oscillation behavior is not modified monotonically by the linear Zeeman interaction. By extracting the fundamental oscillating period T and the amplitude of the induced magnetization with the autocorrelation method [50,51], the period T and the amplitude versus the linear Zeeman field p are demonstrated in Fig. 4. As shown in Fig. 4, in the range of $0 \leqslant p \leqslant 1$, there are four resonant peaks at $p = 0.15, 0.3, 0.56, 0.91$, respectively. Around these resonant fields, the oscillating period and the amplitude are enhanced by several orders. Clearly, Eq. (10) is highly nonlinear and the SOC induced spin-mixing dynamics in the presence of linear Zeeman interaction is quite complicated and requires further investigation in the future.

IV. CONCLUSION

We have investigated the dynamics of the polar bright soliton under the influence of SOC in spin-1 BECs. For small SOC, the system holds the initial soliton structure and polarity. A very weak SOC induces an oscillating dark soliton structure in the other two components with small density distribution, while the oscillation frequency does not depend on the SOC strength. As the SOC becomes comparable with interparticle interaction, the initial bright soliton structure is broken and more particles get transferred to the other two components. At the same time, an additional oscillation at high frequency appears in the system, which is explicitly determined by the SOC strength. Since SOC cannot break the time-reversal symmetry of the system, with the only presence of SOC, the oscillating transition between three components does not destroy the polarity of the system and the system still remains in the polar state. In order to have a nonzero polarization, an additional linear Zeeman interaction is introduced into the system, which leads to the periodic transition of the system from polar state to ferromagnetic state, and a modified oscillation behavior with a more complex frequency dependence.

ACKNOWLEDGMENTS

This work is supported by the National Natural Science Foundation of China (Grants No. 11474138 and No. 11834005), the Program for Changjiang Scholars and Innovative Research Team in University (Grant No. IRT-16R35), and Ministry of Science and Technology of China through Grant No. CN-SK-8-4.

[1] T. Dauxois and M. Peyrard, *Physics of Solitons* (Cambridge University Press, Cambridge, UK, 2006).
[2] R. Carretero-González, D. J. Frantzeskakis, and P. G. Kevrekidis, Nonlinearity **21**, R139 (2008).
[3] F. K. Abdullaev, A. Gammal, A. M. Kamchatnov, and L. Tomio, Int. J. Mod. Phys. B **19**, 3415 (2005).
[4] D. J. Frantzeskakis, J. Phys. A: Math. Theor. **43**, 213001 (2010).
[5] K. E. Strecker, G. B. Partridge, A. G. Truscott, and R. G. Hulet, Nature (London) **417**, 150 (2002).
[6] S. L. Cornish, S. T. Thompson, and C. E. Wieman, Phys. Rev. Lett. **96**, 170401 (2006).
[7] A. L. Marchant, T. P. Billam, T. P. Wiles, M. M. H. Yu, S. A. Gardiner, and S. L. Cornish, Nat. Commun. **4**, 1865 (2013).
[8] L. Khaykovich, F. Schreck, G. Ferrari, T. Bourdel, J. Cubizolles, L. D. Carr, Y. Castin, and C. Salomon, Science **296**, 1290 (2002).
[9] J. H. V. Nguyen, D. Luo, and R. G. Hulet, Science **356**, 422 (2017).
[10] S. Burger, K. Bongs, S. Dettmer, W. Ertmer, K. Sengstock, A. Sanpera, G. V. Shlyapnikov, and M. Lewenstein, Phys. Rev. Lett. **83**, 5198 (1999).
[11] B. P. Anderson, P. C. Haljan, C. A. Regal, D. L. Feder, L. A. Collins, C. W. Clark, and E. A. Cornell, Phys. Rev. Lett. **86**, 2926 (2001).
[12] J. Denschlag, J. E. Simsarian, D. L. Feder, C. W. Clark, L. A. Collins, J. Cubizolles, L. Deng, E. W. Hagley, K. Helmerson, W. P. Reinhardt, S. L. Rolston, B. I. Schneider, and W. D. Phillips, Science **287**, 97 (2000).
[13] Z. Dutton, M. Budde, C. Slowe, and L. V. Hau, Science **293**, 663 (2001).
[14] C. Becker, S. Stellmer, P. Soltan-Panahi, S. Dörscher, M. Baumert, E.-M. Richter, J. Kronjäger, K. Bongs, and K. Sengstock, Nat. Phys. **4**, 496 (2008).
[15] S. Stellmer, C. Becker, P. Soltan-Panahi, E.-M. Richter, S. Dörscher, M. Baumert, J. Kronjäger, K. Bongs, and K. Sengstock, Phys. Rev. Lett. **101**, 120406 (2008).

[16] I. Shomroni, E. Lahoud, S. Levy, and J. Steinhauer, Nat. Phys. **5**, 193 (2009).
[17] A. Weller, J. P. Ronzheimer, C. Gross, J. Esteve, M. K. Oberthaler, D. J. Frantzeskakis, G. Theocharis, and P. G. Kevrekidis, Phys. Rev. Lett. **101**, 130401 (2008).
[18] G. Theocharis, A. Weller, J. P. Ronzheimer, C. Gross, M. K. Oberthaler, P. G. Kevrekidis, and D. J. Frantzeskakis, Phys. Rev. A **81**, 063604 (2010).
[19] P. Engels and C. Atherton, Phys. Rev. Lett. **99**, 160405 (2007).
[20] B. Xiong and J. Gong, Phys. Rev. A **81**, 033618 (2010).
[21] C. Hamner, J. J. Chang, P. Engels, and M. A. Hoefer, Phys. Rev. Lett. **106**, 065302 (2011).
[22] S. Middelkamp, J. J. Chang, C. Hamner, R. Carretero-González, P. G. Kevrekidis, V. Achilleos, D. J. Frantzeskakis, P. Schmelcher, and P. Engels, Phys. Lett. A **375**, 642 (2011).
[23] D. Yan, J. J. Chang, C. Hamner, P. G. Kevrekidis, P. Engels, V. Achilleos, D. J. Frantzeskakis, R. Carretero-González, and P. Schmelcher, Phys. Rev. A **84**, 053630 (2011).
[24] A. Álvarez, J. Cuevas, F. R. Romero, C. Hamner, J. J. Chang, P. Engels, P. G. Kevrekidis, and D. J. Frantzeskakis, J. Phys. B: At., Mol., Opt. Phys. **46**, 065302 (2013).
[25] I. Danaila, M. A. Khamehchi, V. Gokhroo, P. Engels, and P. G. Kevrekidis, Phys. Rev. A **94**, 053617 (2016).
[26] T. M. Bersano, V. Gokhroo, M. A. Khamehchi, J. D'Ambroise, D. J. Frantzeskakis, P. Engels, and P. G. Kevrekidis, Phys. Rev. Lett. **120**, 063202 (2018).
[27] Y.-J. Lin, K. Jiménez-García, and I. B. Spielman, Nature (London) **471**, 83 (2011).
[28] T.-L. Ho and S. Zhang, Phys. Rev. Lett. **107**, 150403 (2011).
[29] H. Hu, B. Ramachandhran, H. Pu, and X.-J. Liu, Phys. Rev. Lett. **108**, 010402 (2012).
[30] C. Wang, C. Gao, C.-M. Jian, and H. Zhai, Phys. Rev. Lett. **105**, 160403 (2010).
[31] K. Sun, C. Qu, Y. Xu, Y. Zhang, and C. Zhang, Phys. Rev. A **93**, 023615 (2016).
[32] C. F. Liu, Y. M. Yu, S. C. Gou, and W. M. Liu, Phys. Rev. A **87**, 063630 (2013).
[33] M. Kato, X. F. Zhang, D. Sasaki, and H. Saito, Phys. Rev. A **94**, 043633 (2016).
[34] M. Salerno, F. K. Abdullaev, A. Gammal, and L. Tomio, Phys. Rev. A **94**, 043602 (2016).
[35] H. E. Nistazakis, D. J. Frantzeskakis, P. G. Kevrekidis, B. A. Malomed, and R. Carretero-González, Phys. Rev. A **77**, 033612 (2008).
[36] P. Szankowski, M. Trippenbach, E. Infeld, and G. Rowlands, Phys. Rev. Lett. **105**, 125302 (2010).
[37] Y. Xu, Y. Zhang, and B. Wu, Phys. Rev. A **87**, 013614 (2013).
[38] L. Li, Z. Li, B. A. Malomed, D. Mihalache, and W. M. Liu, Phys. Rev. A **72**, 033611 (2005).
[39] Y.-K. Liu and S.-J. Yang, Eur. Phys. Lett. **108**, 30004 (2014).
[40] J. Ieda, T. Miyakawa, and M. Wadati, Phys. Rev. Lett. **93**, 194102 (2004).
[41] S. Gautam and S. K. Adhikari, Phys. Rev. A **95**, 013608 (2017).
[42] S. Gautam and S. K. Adhikari, Phys. Rev. A **97**, 013629 (2018).
[43] L. Wen, Q. Sun, Y. Chen, D.-S. Wang, J. Hu, H. Chen, W.-M. Liu, G. Juzeliünas, B. A. Malomed, and A.-C. Ji, Phys. Rev. A **94**, 61602(R) (2016).
[44] X. Antoine and R. Duboscq, Comput. Phys. Commun. **193**, 95 (2015).
[45] Z. F. Xu, Y. Kawaguchi, L. You, and M. Ueda, Phys. Rev. A **86**, 033628 (2012).
[46] Y. Kawaguchi and M. Ueda, Phys. Rev. A **84**, 053616 (2011).
[47] B. Luther-Davies and Y. Xiaoping, Opt. Lett. **17**, 496 (1992).
[48] D. R. Romano and E. J. V. de Passos, Phys. Rev. A **70**, 043614 (2004).
[49] W. Zhang, D. L. Zhou, M.-S. Chang, M. S. Chapman, and L. You, Phys. Rev. A **72**, 013602 (2005).
[50] A. Shukla and S. S. Jibhakate, Int. J. Comput. Appl. **7**, 20 (2010).
[51] The method for obtaining the period by using autocorrelation can be easily implemented in MATLAB. A typical example can be found in the official documentation https://www.mathworks.com/help/signal/ug/find-periodicity-using-autocorrelation.html